AD-A064 586 SHEFFIELD UNIV (ENGLAND) DEPT OF CHEMICAL ENGINEERIN--ETC F/G 21/2
SOME INFRA-RED APPLICATIONS IN COMBUSTION TECHNOLOGY.(U)
1978 J SWITHENBANK, A TURAN, D S TAYLOR AFOSR-74-2682
UNCLASSIFIED HIC-311 AFOSR-TR-79-0006 NL

| OF |
AD
A064586

END
DATE
FILMED
4-79
DDC

H1C 34

LEVEL

department of chemical engineering and fuel technology

UNIVERSITY OF SHEFFIELD

SOME INFRA-RED APPLICATIONS IN COMBUSTION TECHNOLOGY

J. Swithenbank, A. Turan and D.S. Taylor,
Department of Chemical Engineering and Fuel Technology,

Sheffield University, S1 3JD.

165-05

SOME INFRA-RED APPLICATIONS IN COMBUSTION TECHNOLOGY

J. Swithenbank, A. Turan and D.S. Taylor
Department of Chemical Engineering and Fuel Technology,
Sheffield University, S1 3JD.

Abstract

Infrared technology finds many applications in the field of combustion, ranging from pollution monitoring, through military systems, to the control of industrial furnaces and boilers. This review of some selected concepts highlights the interaction between the diagnostic role of infrared measurements and the current status of mathematical modelling of combustion systems. The link between measurement and computing has also evolved to the point where a digital processor is becoming an inherent part of many new instruments. This point is illustrated by reference to the diffraction particle size meter, fire detection and alarm systems, and furnace control. In the future, as fuels become scarce and expensive, and micro-electronics become more available and inexpensive, it is certain that infra-red devices will find increasing application in smaller industries and the home.

Introduction

The continuing availability of energy is one of the most important challenges facing mankind at the present time. Research, development and demonstration of systems which avoid waste during energy conversion is vital if we are to successfully meet this challenge. By the year 2000, it has been estimated that conservation measures could save up to about 30% of the potential national fuel requirements with no loss of amenity[1]. Although nuclear energy will contribute approximately a further 30%, it is clear that combustion of fossil fuels will continue to represent a major part of the energy source. In the short term ($\sim$ 10 years) it is apparent that oil will be a major fuel, and indeed at the present time, about half the world's energy is derived from oil. However, the oil will be largely exhausted by the end of the century whereas the coal reserves will last for many years. It therefore follows that the emphasis in fuel technology will gradually move from oil to coal and coal derived fuels.

It is the responsibility of scientists and engineers to undertake the R,D and D programs which will achieve the rational use of energy, and instrumentation is the key to all phases of this program. Industrial applications of infrared technology in the energy field are therefore largely concerned with combustion and associated conservation techniques.

In this paper, it is not possible to consider all the relevant applications of infrared technology, and therefore only a few selected concepts will be reviewed. These items have been chosen in the hope that some at least will be novel and will stimulate further work in this important and exciting field.

It is currently impossible to discuss combustion and energy without including the minimization of pollutants as an integral part of the study. It is noteworthy that chemical pollutants (CO, NO_x, SO_2, SO_3, dust, smoke) are two or three orders of magnitude more dilute than the species of interest in determining combustion efficiency (CO_2, O_2) and instrumentation systems must be correspondingly more sensitive. However, in research and development, it is not usually sufficient to simply measure the properties of combustion systems, but rather we must compare the results with the predictions of levels and trends, and study how these vary with the geometrical and operating parameters at the control of the designer. The overall result of complementary measurement and prediction is the rational design of optimized combustion systems.

In addition to the stimulus to infrared measuring techniques in combustion caused by concern over energy and pollution, dramatic innovations have been brought about by military incentives. The heat seeking anti-aircraft missile, infrared signature techniques and certain aspects of earth surveillance sattelites are obvious examples of infrared applications involving combustion.

As the gradual oil shortage forces us to move towards fuels with a wider specification and particularly coal derived fuels, it is inevitable that the hydrogen/carbon ratio of the liquid fuel will decrease from the present value of 2 ($\sim$ 20% aromatics for aircraft fuel) to a value approaching 1.5. This change will tend to cause soot to form, which not only increases the smoke pollution problem but also increases radiant heat transfer leading to increased loading in critical boiler regions and increased flame tube temperatures in gas turbine combustors.

Combustor Modelling

Presently the aviation industry produces a wide variety of engine designs, ranging from simple lift engines to sophisticated multispool by-pass engines. In so doing the combustion designer has the important task of selecting the operating conditions which yield maximum efficiency, while minimizing the emission of pollutants. Due to the complexity of the processes involved and consequently lack of fundamental understanding, the designer frequently has to resort to general rules-of-thumb, based on his past experience and qualitative analysis. The rationale behind mathematical modelling is to replace this rule-of-thumb approach by a firmer, quantitative procedure while optimizing a combustor design for any given application.

The technique of mathematical modelling has been the outcome of two disciplines that are apparently independent but complementary in nature. The first of these attempts to solve the differential transport equations for the reacting turbulent continuum using either a finite difference or a finite element technique. This line of approach, with the inclusion of proper physical models and powerful computers, provides

superior combustor predictions of all kinds. The accurate local prediction of two-phase three-dimensional aerodynamic effects and combustion influences is now feasible via such models.

Contrary to the rigorous description employed in the finite difference modelling by partial differential equations of heat, mass and momentum transfer, the "Chemical Reactor Modelling" approach concentrates on the representation of the combustor flow field in terms of interconnected partially stirred and plug flow reactors. This approach has the advantage that the complex, time-consuming solution of the equations is replaced by simple flow models and the computational requirements are generally minimum. These features enable the attractiveness of chemical reactor modelling to be exploited during the development phase of combustor design.

The problem of mathematical modelling combustors is complicated by the fact that the simultaneous processes involved comprise three-dimensional two-phase fluid dynamics, turbulent mixing, fuel evaporation, radiative and convective heat transfer and chemical kinetics. For a model to claim success at all in the prediction of such inter-related phenomena, the above representative processes have to be physically modelled using the findings of previous experimental work. The problems encountered at this stage of modelling stem mainly from the complexity of the laws governing turbulent transport, the chemical kinetics of laminar and turbulent reacting gases, formation and disappearance of condensed-phase particles and thermal radiation through absorbing and scattering media. The other source of difficulty is mathematical in nature and is attributable to the fact that most combustion chamber flows are three-dimensional and the differential equations describing them are numerous, simultaneous and non-linear.

The specific combustor modelling strategy adopted in Sheffield comprises a hybrid approach the first stage of which concentrates on the prediction of hydrodynamic and thermal patterns via a basic finite difference scheme.[2] The pertinent features of turbulence are herein simulated by models incorporating the distribution of kinetic energy of turbulence and its dissipation rate. Spray combustion is computed from the droplet trajectories and evaporation to yield concentrations of the discrete size groups of droplets. Chemical reaction is assumed to proceed in two distinct steps, thereby enabling local concentrations of CO, CO_2, O_2, N_2, H_2O and fuel to be evaluated.

Due to the attractiveness of the flux methods in combined fluid flow and heat transfer predictions, radiation effects (largely infrared) are modelled by reference to the six-flux model of radiation. The differential equations describing the variations of the fluxes are:-

$$\frac{d}{dr}(rI) = r\{-(a+s)I + \frac{J}{r} + aE + \frac{s}{6}(I+J+K+L+M+N)\} \quad (1)$$

$$\frac{d}{dr}(rJ) = r\{(a+s)J + \frac{J}{r} - aE - \frac{s}{6}(I+J+K+L+M+N)\} \quad (2)$$

$$\frac{d}{dx}(K) = -(a+s)K + aE + \frac{s}{6}(I+J+K+L+M+N) \quad (3)$$

$$\frac{d}{ax}(L) = (a+s)L - aE - \frac{s}{6}(I+J+K+L+M+N) \quad (4)$$

$$\frac{d(M)}{rd\theta} = -(a+s)M + aE + \frac{s}{6}(I+J+K+L+M+N) \quad (5)$$

$$\frac{d(N)}{rd\theta} = (a+s)N - aE - \frac{s}{6}(I+J+K+L+M+N) \quad (6)$$

In the above equations the various terms are defined as:

r,θ,x		cylindrical polar co-ordinates.
I,		flux in the direction of positive r.
J,		flux in the direction of negative r.
K,		flux in the direction of positive x.
L,		flux in the direction of negative x.
M,		flux in the direction of positive θ.
N,		flux in the direction of negative θ.
a,		flux absorption coefficient, fraction of radiation absorbed per unit length.
s,		scattering coefficient, fraction of radiation scattered per unit length.
E,	=	σT^4, black body emissive power at the fluid temperature.
σ,		Stefan-Boltzmann constant.

Following previous studies,[3,4] the numerical solution scheme has the pressure and velocities as the main flow variables, and is based on an implicit, upwind finite differencing scheme. (SIMPLE algorithm). The governing equations for the dependent variables are integrated over finite control volumes to derive the finite difference equations which are then solved by a procedure proven to be numerically stable.

Upon obtaining a compatible set of hydrodynamic and thermal fields, the second phase of the prediction procedure, i.e. chemical reactor modelling is initiated. Here attention is focussed on combustion efficiency and pollution levels produced by a particular combustor design using an extensive 17 step kinetic scheme. The basic criterion employed in relating the two stages of the computations is to recognize that mixing at the molecular level is carried out by the movement of molecules between turbulent eddies of different concentrations. Since the molecules also carry momentum and hence dissipate turbulence, it is hypothesized that

mixing rate is proportional to turbulence dissipation rate. The finite difference solution yields the distribution of turbulence dissipation, high values prevailing in the vicinity of the gas jet injections. These regions thus become well stirred reactors of corresponding volume with the degree of stirring or mixing rate factor being determined from the total dissipation within the reactor. Reactors having low mixing rates are represented as plug flow reactors and it is assumed that reactions taking place there are confined to the material which is already mixed. The flow rates and interconnections between the reactors forming the network are determined directly from the overall flow pattern.

The finite difference phase of the above algorithm has been applied to predict the aerodynamic and thermal patterns in a typical gas turbine combustor, Figures 1, 2, 3, for the case of premixed, prevaporized fuel injection. Solution of the pertinent governing equations yields the local distribution of the velocity components, pressure, turbulence quantities, various species mass fractions, temperature and radiation fluxes.

Figure [illegible] display the evolution of the temperature field together with the flux sums, defined as the average value of the two components prevailing at a point, by means of longitudinal and radial profiles.

Particularly noteworthy is the variation of the x-direction fluxes with maximum values lying close to the cylindrical wall. For transverse profiles a minimum is predicted close to the centre-line, while another distinct dip appears midway between the combustor wall and the centre-line. For the particular radial plotting sections employed no significant axial variation is detected in the longitudinal plots.

The axial variation of the y-direction fluxes depicted in figures 8 and 9 clearly indicate the influence of the incoming jets with maximum values lying close to the combustor inlet. The transverse plots on the other hand display monotonically decreasing profiles as the wall is approached.

The z-direction fluxes shown only for longitudinal sections exhibit similar trends to the y-direction fluxes.

Some Infra-Red Diagnostic Techniques in Combustion

Temperature measurements

The measurement of surface temperatures by radiant heat transfer is well established in industry, for example for the measurement of glass and steel temperatures, however it is little used in general research since it is more expensive than a thermocouple and depends on the knowledge of surface emissivity. The hemisperical pyrometer overcomes the latter problem provided the surface can be accessed directly.

Infra-red imaging is a valuable tool in the design and development of furnaces (and other heated structures such as buildings.) However, it should be used in conjunction with mathematical modelling of the structure heat conduction in order to improve the precision of predicting the performance of future designs. In particular, the current swing towards ceramic fibre insulators should be monitored carefully to check both the dynamic response and the effect of insulation anisotropy on furnace design and operation.

With the increasing use of coal in new devices such as the fluidized bed, intriguing problems are posed concerning the respective temperatures of the gas, fluidized solid inerts, and burning coal particles. The rapid response and accurate position information of a two colour I.R. pyrometer suggest that it could be used to resolve such problems. However current observations suggest that only about 10% of the heat is transferred by radiation in a fluidized bed.

Velocity measurement

In order to determine the structure of two phase flames (i.e. liquid or solid particulate fuel), information is required on the velocity, size and trajectory of the particles. In particular, the initial size and velocity of the particles is required for the mathematical modelling of combustors. The gas velocity distribution is also required (among other parameters) in this hot hostile environment, and this can generally be taken as equal to the velocity of particles less than 1 μm.

Laser doppler anemometers are now used routinely to make measurements of the velocities of particles in flames. In this technique, the particles pass through the intersection of two coherent beams of light produced by a laser. In the region of intersection, notional interference 'fringes' are formed which cause the light scattered by the particle to be modulated at a frequency proportional to their velocity. In addition, provided the optics are suitably arranged as shown in Figure 10[5] the envelope of the doppler signal burst can also be used to deduce the size of the particles. Although this technique is normally applied with visible light, there is no fundamental reason why infra-red radiation should not be used similarly.

An alternative technique for the measurement of the size and velocity distribution of particles has also been developed at our laboratory, utilizing a hologram as an intermediate data recording medium[6]. The hologram of the moving particles is made using a double flash ruby laser, in which the 12 ns flashes can be separated by an interval varying from 1 μs to 1 ms. Thus two holographic images of each particle are recorded, separated by a small effective distance depending on the interval and the velocity. The interference fringes observed on reconstruction, Figure 11, can be interpreted directly in terms of the velocity distribution. It is also interesting to note that the particle size distribution can be obtained from the hologram if it is placed in the path of the laser diffraction particle size analyser previously developed at our laboratory.[7] This latter instrument uses a special photo-detector and interfaced computer to rapidly determine the particle size distribution from the Fraunhofer diffraction of a collimated laser beam passed through the particles. Again, this normally uses a laser operating in the red part of the visible spectrum 732.8 nm He/Ne. However the principle would hold for wavelenghts increasing to the microwave band, with the associated feature that the upper size limit of the device would then extend to several cms. A long wave diffraction device such as this could be useful for continuously sizing granulated materials as large as several centimeters.

Identification of Stirred Reactor Networks

In chemical engineering plant design procedure, the concept of the stirred tank reactor and plug flow reactor are frequently used to identify reactors having strong mixing and feeble mixing respectively. In combustors, the well stirred region occurs close to the flame stabilizer, and the system decays to a plug flow reactor when the turbulence dissipation is complete a short distance from the stabilizer. As a result of recirculation and multiple jet entries, a typical combustor can be represented by a network of stirred and plug flow reactors whose volumes and flows must be determined in order to compute the production of pollutants from the chemical kinetic rate equations for the many individual reaction steps occurring as discussed in the modelling section above.

Infra-red measurements can be used to identify the reactor sequence by the pseudo-random test technique in which disturbances are fed to the combustor then the response at the exit plane or various locations within the combustor are monitored. Since only the a.c. response signals are required, a simple infra-red absorption measurement is adequate to monitor the response in terms of concentration of CO, CO_2, etc. The interpretation of the measurements is carried out as follows:-

The output signal from a practical system is almost invariably corrupted with inherent noise in the system. Assuming the validity of linearity, application of superposition yields:

$$Z(t) = y(t) + n(t) \tag{7}$$

where Z(t), y(t) and n(t) represent the output signal, response signal and noise respectively. The mathematical expression relating the process response and the applied input, i(t), is the familiar convolution integral, i.e.

$$y(t) = \int_0^\infty h(t_1)\, i\,(t-t_1)\, dt_1 \tag{8}$$

Here h(t) is the weighting function (or impulse response) of the process.

Combining equations 7 and 8, the measurable output to an arbitrary input signal is given by: (inputs occurring at times greater than T_s in the past are assumed to have no effect on the present output.)

$$Z(t) = \int_0^{T_s} h(t_1)\, i\,(t-t_1)\, dt_1 + n(t) \tag{9}$$

The deconvolution of the above when a short duration pulse is used yields:

$$Z(t) \simeq K_1 h(t) + n(t) \tag{10}$$

where K_1 is a constant determined by the energy in the input pulse. The approximation becomes more accurate as the pulse duration becomes shorter. A step function input yields the step response which is the integral of the impulse response. The effect of noise on the system dynamics represented by n(t) in the above equation can be substantially reduced via correlation techniques.

It can be shown that [8] a relationship exists between the input-output cross-correlation function (ccf) and the input auto-correlation function (acf), i.e.

$$R_{iz}(\tau) = \int_0^{T_s} h(t_i)\, R_{ii}\,(\tau-t_1)\, dt_1 + R_{in}(\tau) \tag{11}$$

(c.f. equation 9)

where $R_{iz}(\tau)$, $R_{ii}(\tau)$ and $R_{in}(\tau)$ represent respectively the input-output ccf, input acf and the input-noise ccf. Assuming $R_{ii}(\tau)$ can be represented by a delta function for random inputs, equation 11 reduces to the following simple form:

$$R_{iz}(\tau) \simeq h(\tau) \tag{12}$$

The practical implementation of a random signal as used in system analysis and identification is a pseudo-random binary signal, PRBS.

The PRBS approximates to a truly random signal due to the properties of its acf. For a periodic PRBS, this can be shown to comprise a series of triangular spikes of width $2\Delta t$ where Δt denotes the bit interval. Furthermore, due to its constant spectral density the PRBS is persistently exciting - a desired quality of the input signal for parameter estimation and identification studies, as the variance of the estimated system parameters is generally proportional to the inverse of the power input.

Amongst the generally available identification techniques including correlation methods, instrumental variables, maximum likelihood, etc, the generalised least squares, GLS, algorithm has proven to be statistically sufficient and is linear in its formulation. The algorithm can provide unbiased estimates, a desirable feature, as data acquired for the formulation of simple dynamic models is almost always corrupted with correlated noise and the need to evaluate unbiased estimates of the process model and of the noise becomes apparent. Additionally, means exist to apply various diagnostic checks.

The algorithm is applied to discrete input/output data sequences i_t, Z_t (t=1 ..... N) to produce optimal models of the form:

$$Z_t = \frac{W^{-k}\, B\,(W^{-1})}{\nabla^p\, A(W^{-1})}\, i_t + \frac{D\,(W^{-1})}{\nabla^p\, C(W^{-1})}\, \xi t \tag{13}$$

where p is the number of integrations in the system and noise models. W represents the forward shift operator and k is the system time delay. ∇ is identified as the differencing operator $(1-W^{-1})$ and A,B,C and D are taken to be polynomials of the form:

$$A(W^{-1}) \equiv 1 + a_1 W^{-1} + \ldots\ldots a_n W^{-n}\ ;\ B(W^{-1}) \equiv b_1 W^{-1} + \ldots\ldots b_n W^{-n}$$

$$C(W^{-1}) \equiv 1 + C_1 W^{-1} + \ldots\ldots C_m W^{-m}\ ;\ D(W^{-1}) \equiv 1 + d_1 W^{-1} \ldots\ldots d_m W^{-m} \tag{14}$$

In equation 13 the rational transfer function driven by the uncorrelated sequence ξ_t comprises the entire extraneous behaviour.

Equation 13 can be re-expressed upon removal of the system integrations by data differencing in the following convenient form:

$$AZ_t = W^{-k}\, Bi_t + \frac{AD}{C}\, \xi_t \tag{15}$$

It is worth noting that unless $ADC^{-1} \equiv 1$, the process parameter estimates will be biased. Hence the GLS aims to transform the term $ADC^{-1}\xi_t$ iteratively to an uncorrelated sequence ξ_t via the following steps:

i) The process parameters (a_i, b_i) are initially estimated by an ordinary least squares.

ii) The residuals, viz,

$$e_t = \hat{A}Z_t - W^{-k}\,\hat{B}i_t \tag{16}$$

($\hat{}$ denotes estimated values)

are analysed to be subsequently transformed by autoregression.

$$\hat{F}\, e_t = \xi_t$$

iii) The process input and output are filtered with the autoregression $\hat{F}$ to yield:

$$Z_t^F = \hat{F}Z_t \tag{17}$$

$$i_t^F = \hat{F}i_t \tag{18}$$

iv) i_t^F and Z_t^F are modified by a new least squares fit to commence another iteration cycle proceeding from step ii. The final model is expressed in the form:

$$\hat{A}(\hat{F}Z_t) = W^{-k}\,\hat{B}\,(\hat{F}i_t) + \xi_t \tag{19}$$

The validity of the estimated process and noise models given by the GLS algorithm have to be established by diagnostic checks for the statistical properties of the models. Currently available diagnostic algorithms utilize model order tests including determinant-ratio test, F-ratio test, loss function analysis, pole-zero cancellation and tests for independence. In addition, auto-correlations of the residuals and cross-correlations of the input and the residuals can be employed to reveal the adequacy of the fitted model.

Tentative values for the time delay and model order can be obtained via the impulse response evaluated directly by cross-correlation of the input and output for white inputs, equation 10. An alternative means of extracting the same information is to use the determinant ratio tests [9]. The test is especially valuable in that it limits the number of possible model orders and associated time delays prior to parameter estimation if the signal to noise ratio is reasonably high.

Loss function analysis and the associated F-ratio test are employed once the process and noise models have been derived by the GLS algorithm. They are primarily concerned with the behaviour of the error function in the neighbourhood of N_o, taken to correspond to the actual system order.

Additionally, residual manipulation in terms of acf's and ccf's provides a critical assessment of the structure and order of the estimated model. The acf of the residuals is employed to yield an indication of the measure of the whiteness of the residuals. The ccf, on the other hand establishes the statistical independence of the residuals and the process input.

The above ideas have not yet been applied using infra-red diagnostics, however using a tracer technique they have been applied comprehensively to study the isothermal residence time distributions in the Lycoming combustor with the objective of quantifying the stirred and plug flow reactor locations. The predicted aerodynamic patterns yielded by the finite difference procedures are utilized in conjunction with the GLS algorithm to determine the local mixing history. A detailed description of the experimental set up and the measuring environment is given in [10].

The investigation employed PRBS and step signals respectively as the system mode of excitation for parameter estimation purposes. The particular PRBS adopted comprises a period 15, bit interval 1.1 sec and amplitude ±1volts, to a solenoid valve introducing the tracer. A number of measuring stations, representative of the distinct mixing zones in the combustor, were chosen for identification and parameter estimation. A typical sequence of operational steps adopted in such an analysis is summarized as follows:

A determinant ratio test was employed to limit the number of possible model orders for the range of time delays suggested by the deconvoluted impulse response. GLS parameter estimation was then applied for varying model orders and time delays. The optimum value for the latter was taken as that which minimised the sum of squared residuals. Typically noise model orders of 10-15 were adopted in an iterative scheme of 5-10 steps. The loss function was recorded for all the different cases tried.

Diagnostic checks comprising mainly the evaluation of the acf of the residuals, ccf between the input sequence and the residuals and pole-zero cancellation were applied for varying model orders and time delays. Parameter estimation and subsequent validation was carried out in a strict iterative manner. Finally the impulse response function corresponding to the estimated model was computed and this was compared with the original weighting sequence obtained from the cross-correlation analysis of the input/output data.

Figure 12 displays waveforms labelled modified output and deterministic prediction errors. These respectively refer to the system response resulting from the preliminary data transformations (normalising, trend removal, editing, etc.) and the computational mismatch between the predicted and measured outputs.

The analysis reveals that the measuring station, immediately below the incoming primary jets, can be modelled as a second order system with a time delay of 1. These findings are quantitatively supported by the excellent agreement observed between the predicted and measured pulse responses, Figure 13. Thus the system response is identifiable by a transfer function having the parameters as:

$$a_i = -0.7527 \quad , \quad -0.1179$$

$$b_i = 3.157 \quad , \quad 116.5 \quad .$$

Fire detection

It is well known that fires emit copious quantities of infra-red radiation, which, in principle can be used for the detection of unintentional fires. A common problem with alarm systems of this type is the difficulty of distinguishing between real fires and false alarms. False alarms can arise, for example from reflected sun-light, and the electronic system associated with the alarm often attempts to eliminate this possibility by selecting signals modulated at the characteristic flicker frequency associated with Rayleigh-Taylor instability of the flame. Nevertheless, there are situations such as sunlight reflected from the moving ocean surface where this is not successful and an alternative must be sought. The evolution of the micro-processor now provides an important new signal processing capability to detection systems. A novel application is to combine the signals from two or more detectors, which scan the scene of interest mechanically, optically or electronically, to compute the two or three-dimensional location and size of the fire. If the 'fire' results from a solar reflection, or some other source outside the region of interest the alarm is not raised. Such a system can also be 'taught' interactively to ignore intentional fires or other radiation sources in any particular section of the overall region. The associated display system can also pinpoint the location of the fire and, if necessary, take selective action to extinguish it. The protection of department stores, warehouses and even oil rigs by such a system opens dramatic new prospects in infra-red applications technology.

An interesting result from some of our recent research on oil tank farm fires shows that they are strongly affected by the air flow around the tank resulting from cross-wind. This is important since the average cross-wind at a tank farm is about 6 metres/second. Since the inertial forces of the air are larger than the flame buoyancy force, the flame tends to be drawn down into the counter-rotating vortices in the wake of the tank. Adjacent tanks and equipment are often located in this region, and it follows that they will be subjected to ignition sources and strong convective heating in addition to the radiant heat transfer from the plume. As pointed out above, mathematical modelling procedures have now advanced to the point where these complex three dimensional reactive flow fields can be predicted, permitting accurate estimates of the heat transfer by solving the relevant differential equations simultaneously and integrating all the radiation contributions.

Window design

With the increasing use of optical diagnostic techniques, we are often faced with the problem of window design. One of the simplest techniques in hot (flames) environments is to use an uncooled plastic (plexiglass) window. This ablates away thus cooling itself naturally. On a typical rocket motor operating at 100 ats, 3000°K the window ablates about 0.2 mm/sec. and it is relatively simple and cheap to replace the inner 6 mm thick window after each firing.

If the distortion introduced by ablating windows cannot be tolerated, e.g. in L.D.A. systems, then quartz windows are recommended. Often it is necessary to protect the surface from fuel sprays and other deposits and a screening layer of clean gas must be used. In this case it is important that the gas is introduced through wide, low speed jets at the edge of the window. The jet will protect the window for its potential core length (~ 10 slot widths) as shown in Fig. 14. Beyond the potential core, in the mixing region, the window can easily become contaminated from the entrained material.

Optical computers

With modern microcircuits, the speed of data processing has become remarkably fast, for example, current state of the art circuitry will permit a special purpose built circuit to obtain a one-dimensional Fourier transform at 128 points in 30 microseconds. However, optical computers can operate at least 1000 times faster (see Table 1) and for some particular applications they offer distinct advantages. The mathematical operations which they can perform readily are two-dimensional Fourier transformation (as demonstrated by the

laser diffraction particle size distribution meter discussed above), two-dimensional cross-correlation and two-dimensional convolution functions. Figure 15 shows the typical arrangement of lenses to achieve these operations. Since the operations which can be carried out by an optical computer are limited, it is usually necessary to combine an optical computer with a digital processor to achieve an overall system.

Combustion Control

The aim of an automatic mixture ratio control system is to maintain the fuel and air supplies to a boiler or furnace in the correct proportions. The correct ratio between the fuel and air is usually attained when there is just sufficient air to ensure complete oxidation of the fuel under the conditions existing in the furnace. Any mixture ratio control system should be judged on the closeness with which it approaches this ideal in steady and unsteady state conditions.

If mixture ratio control could be fitted to all the combustors in the U.K., the benefit to the country in terms of cost of fuel saved would be about £1000 p.a. plus the advantage of mitigating the iminent energy shortage. There is therefore considerable incentive to utilize or develop an economic and reliable combustion control system. Visits to any but the largest burner installations will soon show that most present monitoring and control instrumentation is unreliable or unused. It is not within the scope of this paper to survey the features of all combustion control systems, however the characteristics of some systems involving infra-red devices will be discussed.

If the furnace is generally operated in steady state the response of the control system does not need to be particularly fast and exhaust gas sampling systems can be used. Carbon monoxide measurements using an infra-red absorption instrument, usually of the non-dispersive type, are commonly used to provide the control signal, and the carbon monoxide level is maintained at some acceptably small value. The problems with such a system are largely; the need for calibration of the instrument; sampling problems due to the fact that carbon monoxide concentration is far from uniform across the flue; the problem of matching individual burners on a multi-burner installation; soot, water and other deposits in the sample line; air in leakage in the furnace or sample system; accumulated soiling of the sample chamber windows; operation and 'maintainence' by unskilled operators; and finally, the cost of proper maintainence which quickly exceeds the cost of any fuel saving. The overall experience and economics has therefore acted against the installation of fuel/air ratio controls on smaller systems in spite of the potential benefit.

Carbon dioxide measurements can also be based on infra-red absorption, however the concentration vs. fuel/air ratio characteristic becomes relatively flat in the vicinity of stoichiometric mixtures and it does not therefore provide a very good control signal.

An interesting control signal can be derived from the flame radiation. Since the band radiation is proportional to the concentration of the emitting species multiplied by approximately the fourth power of the temperature, both of which peak close to stoichiometric mixtures, one has a signal with a pronounced peak as a function of fuel/air ratio, and a peak-seeking feedback control system can easily locate this peak even in the presence of noise. In the case of a natural gas flame the major emitters are CO_2 and H_2O whose infra-red bands carry most of the radiated energy. Provided the mixing time in the flame is small compared with the kinetic time, which is true for all high intensity gas burners for both pre-mixing or nozzle-mixing systems, the peak is quite reliable. However, if the flame is operating as a slow, non-premixed diffusion flame, then, as with a candle flame, the air fuel ratio cannot be defined, and a peak seeking system cannot be used.

With oil or coal flames, most of the radiant energy is due to luminous soot in the flame and the radiation depends primarily on the fourth power of the soot (i.e. flame) temperature and non-linearly on soot concentration. In this case, again neglecting diffusion type flames, the peak in radiation occurs, however it is now at the soot emission boundary. That is, if the flame is operated any leaner the flame temperature drops due to excess air, whilst any richer results in the flame temperature dropping due to the emission of unburned agglomerated soot from the burner. The radiation peak therefore usually corresponds to the desirable operating point of the burner. This point is usually closer to stoichiometric when the burner is operating at full load than when it is operating at low load.

It is interesting to note that a peak seeking detection system does not need calibration, is insensitive to dirty windows, and can readily identify individual burners in a multi-burner installation.

With the advent of cheap digital processors, it is now possible to operate the burner at any required air/fuel ratio away from the peak, with only occasional excursions to the peak to obtain its location. Such systems can also attend to light-up and operate several system simultaneously. An interesting feature is that they can 'remember' and periodically update (as necessary) the optimum air and fuel valve settings for any demanded heat output and thus an optimally fast feedforeward/feedback control characteristic can be obtained for dynamic load following.

Conclusions

We feel a burning enthusiasm for digital processors in combustion diagnostics and foresee that the future is particularly bright for infra-red systems.

References

1. Swithenbank, J. et al,"The Rational Use of Energy," Watt Committee Report No.3. Watt Committee, 1, Birdcage Walk, Westminster, London. SW1H 9JJ.

2. Swithenbank, J., Turan, A., Felton, P.G.,"3-Dimensional 2-Phase Mathematical Modelling of Gas Turbine Combustors," Presented at SQUID Workshop, Purdue University, 1978.

3. Patankar, S.V. and Spalding, D.B., "A Calculation Procedure for Heat, Mass and Momentum Transfer in Three-Dimensional Parabolic Flows", Int. Journal of Heat and Mass Transfer, 15, 1972.
4. Patankar, S.V. and Spalding, D.B., "Simultaneous Predictions of Flow Patterns and Radiation for 3-Dimensional Flames", Heat Transfer in Flames, Edited by N.H. Afgan and J.M. Beér, Scripta Technica, 74, 1975.
5. Chigier, N.A., Ungut, A., Yule, A.J., "Particle size and velocity measurement in flames by laser anemometer", 17th. Symp. (Int) on Combustion, Leeds, 1978.
6. Ewan, B.C.R., "Holographic particle velocity measurement in the Fraunhofer Plane", Dept. of Chemical Engineering and Fuel Technology, Sheffield University, Report No. HIC 296, July 1978.
7. Swithenbank, J. et al., "A laser diagnostic technique for the measurement of droplet and particle size distribution". Experimental Diagnostics in Gas Phase Combustion Systems. Progress in Astronautics and Aeronautics. Vol. 53 AIAA, 1977.
8. Lee, Y.W., "Statistical Theory of Communication", John Wiley and Sons, 341, 1960.
9. Billings, S.A., Ph.D. Thesis, University of Sheffield, 1975.
10. Turan, A., Ph.D. Thesis, University of Sheffield, 1978.

Acknowledgements

Financial support for this work has been received from the Science Research Council and the USAF European Office of Scientific Research under Grant No. 74 - 2682. This support is gratefully acknowledged. The authors also wish to acknowledge the valuable discussions with Professor Spalding who also made the basic finite difference program available to us. The contribution of CHAM is acknowledged.

Rate bits/sec	Image Production	Transmission	Storage	Processing
10^{12}	High Speed Photography	Optical Image (Short distance)	High Speed Photography	Optical Computer
10^{11}				
10^{10}				
10^{9}	Eye	Laser beam	High Speed Core	High Speed Computer
10^{8}	Colour TV B/w TV	TV channel Data link	Video tape	Medium Speed Computer
10^{7}	100 x 100 array			
10^{6}	Radar	Hifi	Mag. disc	
10^{5}	Facsimile	Voice Telephone	Mag. tape Fast printer	
10^{4}			Paper tape reader	Calculator
10^{3}		Human Reader	Paper tape punch	
10^{2}		Teletype	Writing	Hand Calculation

Table 1.

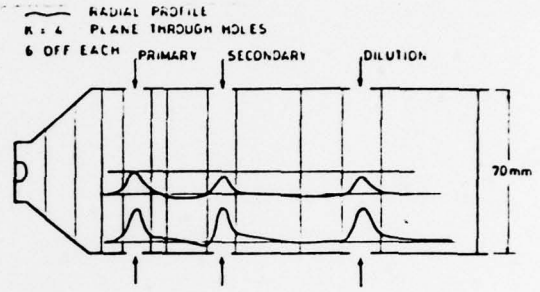

Fig. 1. Predicted Radial Velocity Profiles (Axial Cross-section) for the Lycoming Combustor. (Isothermal, K = 4)

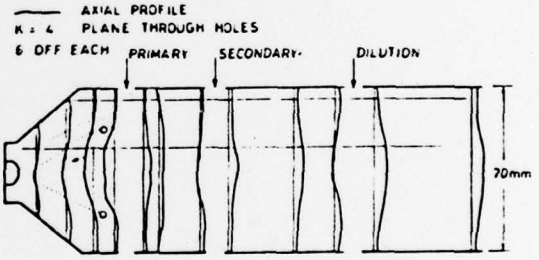

Fig. 2. Predicted Axial Velocity Profiles (Axial Cross-Section) for the Lycoming Combustor, (Isothermal, K = 4)

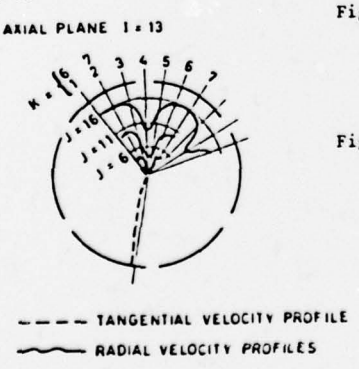

Fig. 3. Predicted Radial and Tangential Profiles (Transverse Cross-Section) for the Lycoming Combustor, (Isothermal, I = 13)

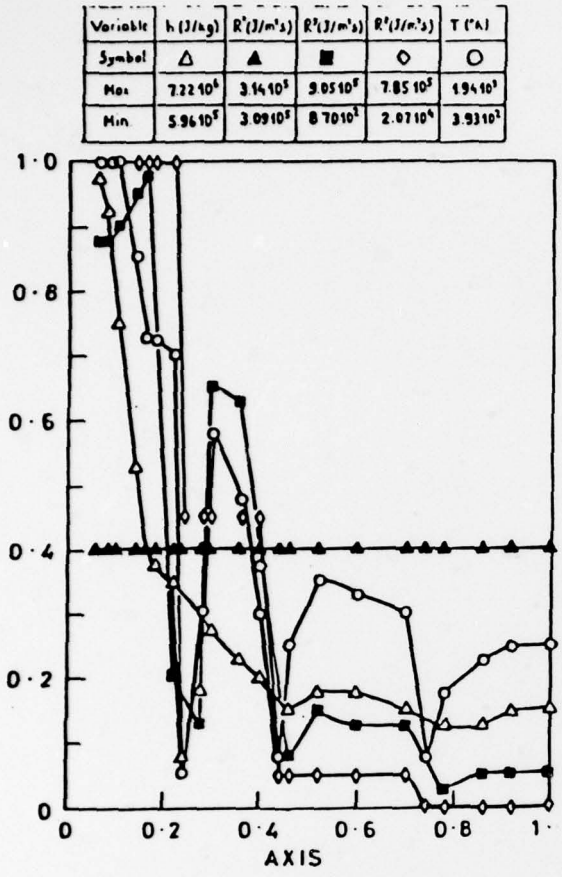

Fig. 4. Predicted Longitudinal Thermal Profiles For the Lycoming Combustor, K = 4, J = 10.

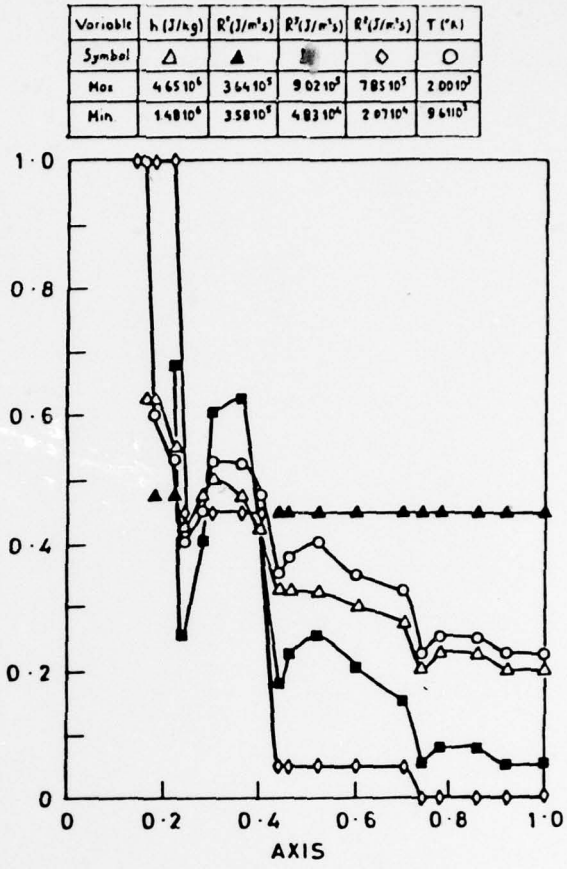

Fig. 5. Predicted Longitudinal Thermal Profiles for the Lycoming Combustor, K = 5, J = 17.

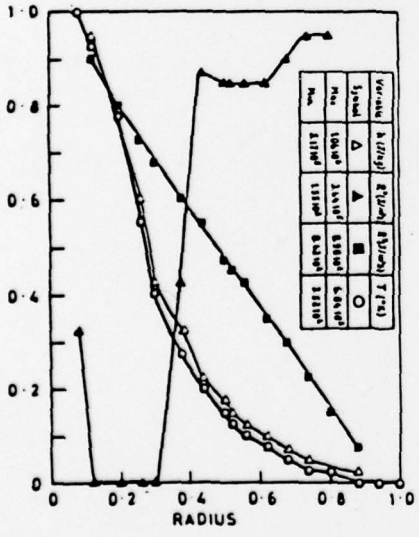

Fig. 6. Predicted Transverse Thermal Profiles for the Lycoming Combustor, K = 4, I = 13.

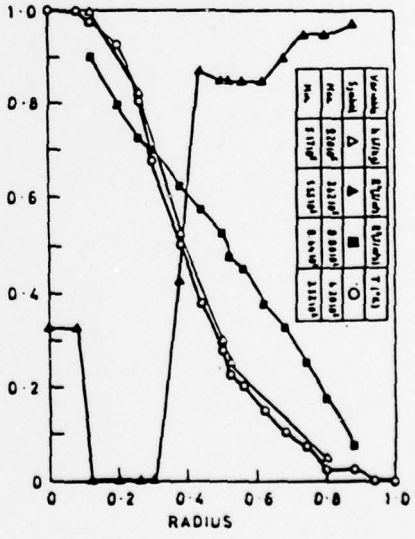

Fig. 7. Predicted Transverse Thermal Profiles for the Lycoming Combustor, K = 4, I = 18.

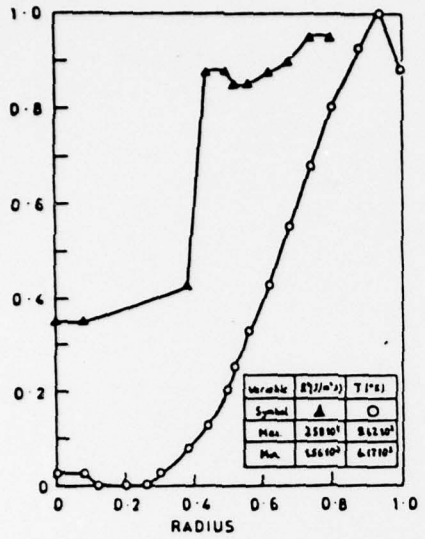

Fig. 8. Predicted Transverse Thermal Profiles for the Lycoming Combustor, K = 4, l = 27.

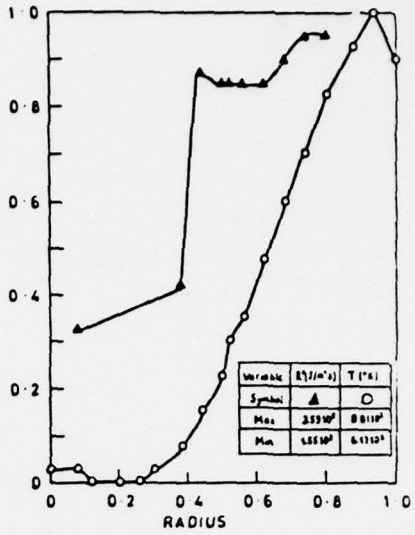

Fig. 9. Predicted Transverse Thermal Profiles for the Lycoming Combustor, K = 5, l = 27.

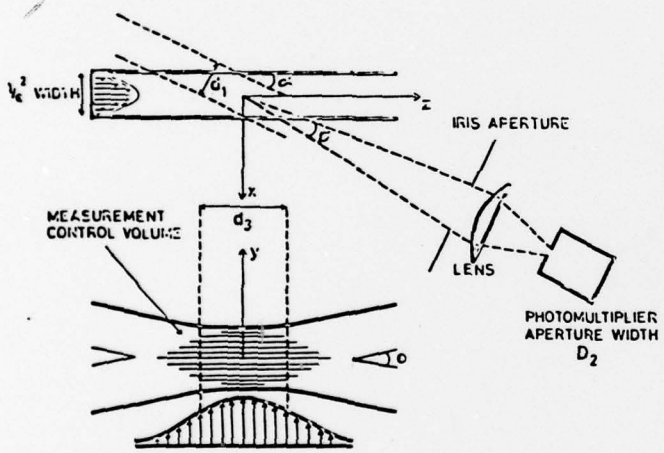

Fig. 10. Dimensions of the Control Volume with 'off axis' collection geometry.

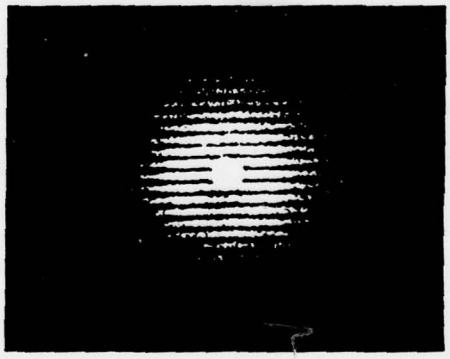

Fig. 11. Fringe Patterns in the Fraunhofer Plane.

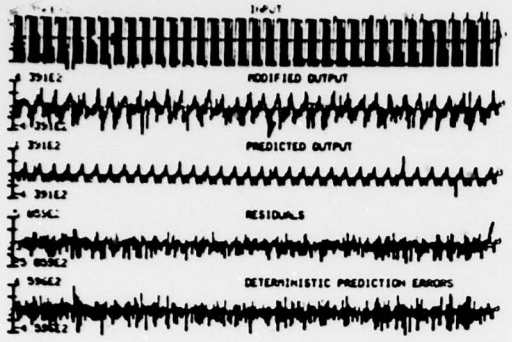

Fig. 12. Estimated Model for Position 13 Together with Auxilliary Waveforms.

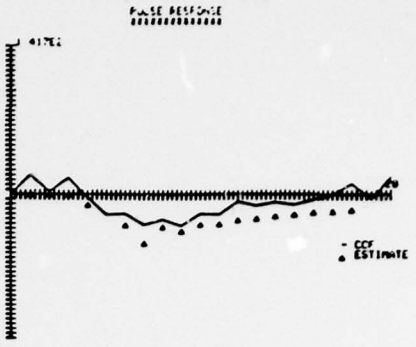

Fig. 13. Comparison Between the Predicted and Measured Pulse Responses for Position 13.

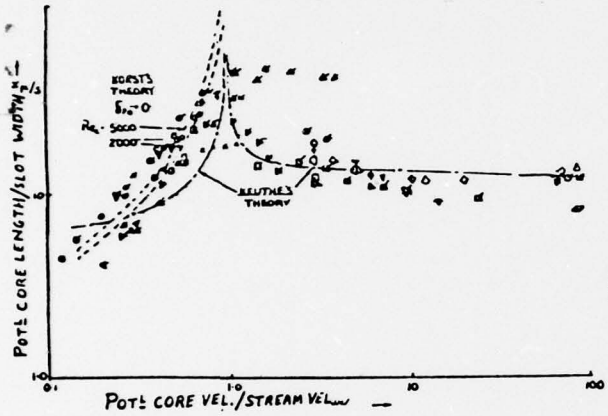

Fig. 14 Potential Core/Slot Height vs Core Velocity/Stream Velocity.

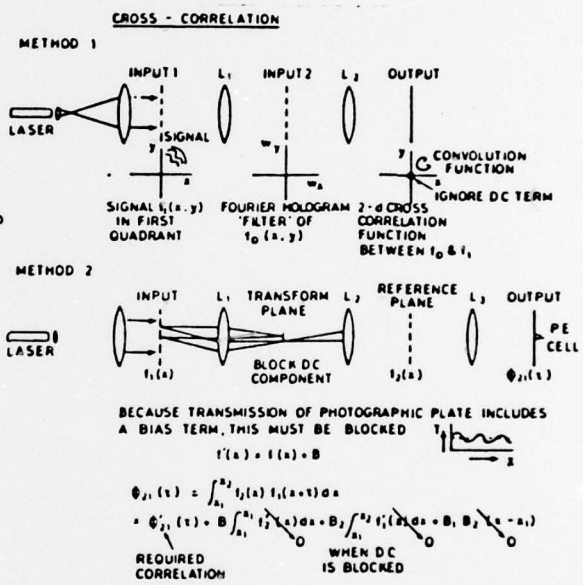

Fig. 15. Optical Computer Systems.

UNCLASSIFIED

SECURITY CLASSIFICATION OF THIS PAGE (When Data Entered)

REPORT DOCUMENTATION PAGE

READ INSTRUCTIONS BEFORE COMPLETING FORM

1. REPORT NUMBER: AFOSR-TR-79-0006	2. GOVT ACCESSION NO.
3. RECIPIENT'S CATALOG NUMBER	
4. TITLE (and Subtitle): SOME INFRARED APPLICATIONS IN COMBUSTION TECHNOLOGY	5. TYPE OF REPORT & PERIOD COVERED: INTERIM rept. 1 Mar 78 — 31 Aug 78
6. PERFORMING ORG. REPORT NUMBER	
7. AUTHOR(s): J. SWITHENBANK, A. TURAN, D. S. TAYLOR	8. CONTRACT OR GRANT NUMBER(s): AFOSR-74-2682
9. PERFORMING ORGANIZATION NAME AND ADDRESS: UNIVERSITY OF SHEFFIELD, MAPPIN ST, SHEFFIELD S1 3JD	10. PROGRAM ELEMENT, PROJECT, TASK AREA & WORK UNIT NUMBERS: 2308A2, 61102F, A2
11. CONTROLLING OFFICE NAME AND ADDRESS: AIR FORCE OFFICE OF SCIENTIFIC RESEARCH/NA, BLDG 410, BOLLING AIR FORCE BASE, D C 20332	12. REPORT DATE: 1978
	13. NUMBER OF PAGES: 12 (15 p.)
14. MONITORING AGENCY NAME & ADDRESS (If different from Controlling Office): HIC-311	15. SECURITY CLASS. (of this report): UNCLASSIFIED
	15a. DECLASSIFICATION/DOWNGRADING SCHEDULE

16. DISTRIBUTION STATEMENT (of this Report)

Approved for public release; distribution unlimited.

17. DISTRIBUTION STATEMENT (of the abstract entered in Block 20, if different from Report)

18. SUPPLEMENTARY NOTES

19. KEY WORDS (Continue on reverse side if necessary and identify by block number)

STIRRED REACTORS
MODELLING
INFRARED
COMBUSTION DIAGNOSTICS
MATHEMATICAL MODELLING

20. ABSTRACT (Continue on reverse side if necessary and identify by block number)

Infrared technology finds many applications in the field of combustion ranging from pollution monitoring, through military systems, to the control of industrial furnaces and boilers. This review of some selected concepts highlights the interaction between the diagnostic role of infrared measurements and the current status of mathematical modelling of combustion systems. The link between measurement and computing has also evolved to the point where a digital processor is becoming an inherent part of many new instruments. This point is illustrated by reference to the diffraction particle size meter, fire detection and alarm

DD FORM 1 JAN 73 1473

400877

UNCLASSIFIED

SECURITY CLASSIFICATION OF THIS PAGE (When Data Entered)

systems, and furnace control. In the future, as fuels become scarce and expensive, and micro-electronics become more available and inexpensive, it is certain that infrared devices will find increasing application in smaller industries and the home.